CONF-970503--11
DOE/ER/40150--1120

JLAB-ACP-97-01

RECEIVED
JUN 17 1997
OSTI

Lattice Design for a High-Power Infrared FEL

D. R. Douglas, Thomas Jefferson National Accelerator Facility,
12000 Jefferson Avenue, Newport News, VA 23606-1909 USA

Abstract

A 1 kW infrared FEL, funded by the U.S. Navy, is being built at Jefferson Lab. It will be driven by a compact energy-recovering CW superconducting radio-frequency (SRF)-based linear accelerator. Stringent phase space requirements at the wiggler, low beam energy, and high beam current subject the design to numerous constraints. This report addresses these issues and presents a design solution for an accelerator transport lattice meeting the requirements imposed by physical phenomena and operational necessities.

1 PROJECT OVERVIEW

The U.S. Navy is sponsoring construction of a high-power FEL at Jefferson Lab. Driven by a compact, SRF-based energy-recovering CW linac (parameters of which are in Table 1), it will produce a 1 kW, 3–6.6 μm photon beam.

Table 1: Driver Accelerator Parameter List

Injection kinetic energy	10 MeV
Beam kinetic energy at wiggler	42 MeV
Beam kinetic energy at dump	10 MeV
Beam current	5 mA
Normalized rms emittance, design:	13 mm-mrad
nominal:	5 mm-mrad
FEL extraction efficiency	0.5 %
$\delta p/p$, rms at wiggler	0.5 %
full after wiggler	5 %

The driver accelerator comprises a 10 MeV injector, a linac based on a single Jefferson Lab cryomodule containing eight SRF cavities, a wiggler and optical cavity, and an energy-recovery recirculation arc (to limit cost and technical risk by reducing RF power requirements in the linac). Construction ends in October 1997; operations follow immediately to produce first light by February 1998. High-power end-user service commences in summer 1998. The U.S. Navy funding contribution is $8.1 million; further project and design information are available elsewhere in these proceedings [1] and on the World Wide Web as a link from http://www.jlab.org/.

2 DESIGN REQUIREMENTS

2.1 *Fundamental Requirements*

The driver transport system must meet two fundamental requirements. First, it must deliver to the FEL an electron beam with a properly configured phase space. Second, it must transport the "spent" beam from the wiggler back through the accelerating structure for energy recovery.

The first requirement is imposed by the FEL system [2], which is based on a cavity resonator with low (~1/2%) extraction efficiency and modest instantaneous power output. High average output power is achieved by using a high repetition rate; this avoids many of the difficulties of low-rep-rate, high-peak-power systems. The FEL is optimized to use a 42 MeV, 5 mA beam of 135 pC bunches delivered at 37.425 MHz; a beam with normalized rms emittance below 13 mm-mrad and $(\delta p/p)_{rms}$~0.5% is required. Electron beam/optical mode overlap requirements demand betatron matching into the wiggler; the peak current needed for the design FEL gain requires longitudinal phase space management by bunch length compression to an rms length of ~1 psec at the wiggler.

The second requirement embodies the use of energy recovery to reduce RF power demands, cost, and radiation effects by using the recirculated beam to drive the RF cavities. As the full momentum spread after the wiggler will be 5%, this creates a need for large transport system acceptance.

2.2 *Physical Phenomena/System Constraints*

These requirements couple to many physical phenomena and constraints. The system design must be simple and economical to meet cost and schedule constraints. Low instantaneous FEL power and high repetition rate suggest use of a CW driver; the project time scale leads to use of standard Jefferson Lab SRF components. Transverse matching and longitudinal phase space management requirements at the wiggler imply quadrupole telescopes and a bunch length compressor are needed. High current and low energy suggest collective effects may be important. To avoid space-charge-driven beam quality degradation, a moderately high injection energy is needed [3]. Beam breakup (BBU) and other impedance-driven instabilities must be avoided [4]. Coherent synchrotron radiation (CSR) must be managed to preserve beam emittance [5]. RF stability must be assured, particularly in transient regimes such as FEL turn-on and initiation of energy recovery [6].

The energy-recovery transport must have large acceptance to limit beam losses from a 5% momentum spread beam. Control of beam envelopes and lattice aberrations must be provided over a large volume of phase space. Variable momentum compaction is needed to allow energy compression and optimization of RF stability during energy recovery. This reduces the momentum spread, and enhances the stability, of the 10 MeV energy-recovered beam during transport to the dump.

Project constraints and physical effects eliminate most candidate system configurations. Jefferson Lab cryomodules cannot simultaneously accelerate (decelerate) two

DISTRIBUTION OF THIS DOCUMENT IS UNLIMITED
HH
MASTER

DISCLAIMER

This report was prepared as an account of work sponsored by an agency of the United States Government. Neither the United States Government nor any agency thereof, nor any of their employees, make any warranty, express or implied, or assumes any legal liability or responsibility for the accuracy, completeness, or usefulness of any information, apparatus, product, or process disclosed, or represents that its use would not infringe privately owned rights. Reference herein to any specific commercial product, process, or service by trade name, trademark, manufacturer, or otherwise does not necessarily constitute or imply its endorsement, recommendation, or favoring by the United States Government or any agency thereof. The views and opinions of authors expressed herein do not necessarily state or reflect those of the United States Government or any agency thereof.

DISCLAIMER

Portions of this document may be illegible in electronic image products. Images are produced from the best available original document.

beams moving in opposite directions due to constraints on RF phases in adjacent cavities. Use of existing hardware designs (to meet cost and schedule goals) therefore excludes any geometry accelerating and energy recovering with anti-parallel beams. Concepts using multiple cryomodules or custom RF components are eliminated by cost.

FEL placement in the system is dictated by the relative importance of various physical phenomena. Partial or complete recirculation before the wiggler avoids transport of the large momentum spread "spent" beam, simplifying energy recovery but leaving CSR- and space-charge-driven emittance growth as a potential problem. We therefore locate the FEL immediately downstream of the linac. This choice reduces the impact of CSR and space charge, at a possible cost of increased complexity in the energy recovery transport. It also allows for "straight-ahead" operation of the machine (without energy recovery) to drive the FEL at low powers during initial operation.

3 DESCRIPTION OF SOLUTION

3.1 Detailed System Design Specifications

The design concept (Figure 1) comprises a 10 MeV injector, a single eight-cavity Jefferson Lab cryomodule accelerating to 42 MeV, transport to the wiggler, and energy-recovery transport from wiggler through module to a beam dump. Specifications exist for each of these segments. The module-to-wiggler transport must provide transverse matching and bunch length compression. The energy-recovery transport must have large momentum acceptance (>5%) and variable momentum compaction (similar in magnitude to that of the module-to-wiggler compression).

Other specifications are global. Beam spots and envelopes should be modest throughout the system ($\beta < 25$–30 m). Components must be simple, robust, low cost, and, if possible, in the Jefferson Lab inventory. As the beam energy is low, dipoles will bend through large angles and focus strongly; the effects of dipole edges, gaps, and field rolloff must be incorporated in design computations. Finally, the system should avoid aggravating collective effects such as CSR, BBU, space charge, or other instabilities.

3.2 Transport to the Wiggler

A four-quadrupole telescope in the injector provides betatron matching into the driver linac; an achromatic line transports beam from the telescope to the linac axis. The linac comprises a single high-gradient cryomodule, and accelerates the beam by 32 MeV. RF focusing controls the beam envelopes; the beam will be accelerated 12.5° off crest, so as to slew the longitudinal phase space in preparation for bunch length compression before the wiggler.

After the cryomodule, a quadrupole telescope (two triplets) betatron matches the beam to the wiggler. An achromatic four-dipole chicane between the triplets separates optical cavity and electron beam components while compressing the bunch length. The chicane geometry is limited by the allowable momentum compaction. Larger chicanes provide more space, but lead to higher momentum compactions and more jitter in time of flight; to maintain FEL pulse/electron beam synchronism with the available RF stability, the momentum compaction must be modest ($|M_{56}| < 0.3$ m).

Studies indicate space charge is not important in full-energy segments of the system [7]; single-particle design tools can be used for the 42 MeV transport. Space charge does, however, affect motion in the injector and the module. Injection matching and the beam phase space just after the module thus depend on current. The machine will use a fixed single-bunch charge (60 pC for first light, 135 pC for full power), and vary the average current by altering the repetition rate. Wake-field effects will be small, so space charge effects will not be dependent on repetition rate, but only on the bunch charge. A separate solution for the injector-to-module and module-to-wiggler matches will therefore be used for each bunch-charge state.

3.3 Energy-Recovery Transport

After the wiggler, the electron beam (with a full momentum spread of ~5%) is transported through a recirculation arc to the cryomodule for energy recovery. A second six-quadrupole telescope is used to betatron match into the recirculation arc. This avoids beam envelope mismatch, large spot sizes, aggravated optical aberrations, error sensitivities, and potential beam loss. As in the transport to the wiggler, a dipole chicane embedded in the telescope moves the electron beam around the optical cavity; this chicane lengthens bunches, reducing peak currents and alleviating potential space charge and CSR effects.

The transport arc is an isochronous, large-momentum-acceptance beamline based on the MIT/Bates Linear Accelerator Center recirculator [8]. Dipole parameters

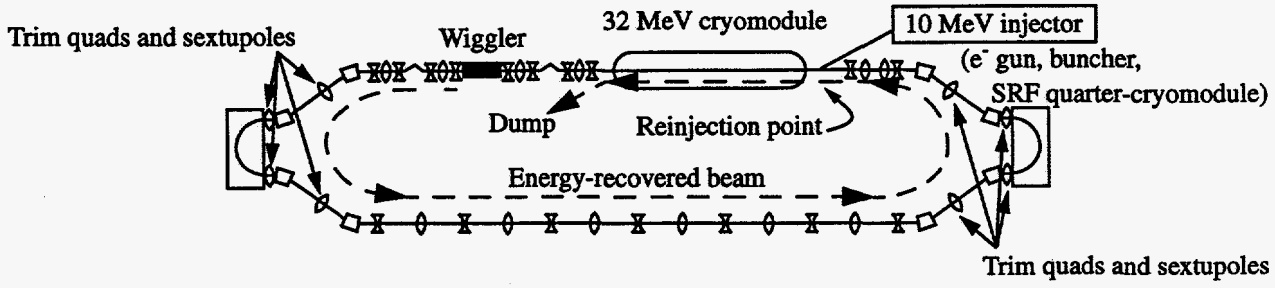

Figure 1: Design concept for Jefferson Lab 1 kW IR FEL driver accelerator.

(bend and edge angles) and drift lengths are set to provide M_{56}=0 from wiggler to reinjection point, and, across each end loop, achromatic, betatron stable motion in x (with a tune of 5/4) and imaging transport (M_y=-I) in y. The end loops are joined by six 90° FODO cells. $M_{x,y}$=-I over the backleg, giving M_x=I and M_y=-I and, with reflective symmetry about the center of the backleg, suppression of aberrations over the full arc. The symmetry giving this suppression can be imposed due to the choice of wiggler placement immediately after the linac. Each end loop has four trim quads for dispersion and compaction control; M_{56} can be varied over ±0.25 m. Each also has four sextupoles to suppress aberrations. T_{166}, T_{266}, and T_{566} are set to zero; others are controlled by the choice of system parameters. The system path length is nominally 501.5 RF wavelengths; this can be varied by ±1/2 wavelength by trim steering in the 180° bends.

After the beam is returned to the linac axis, a four-quad telescope matches it into the module for energy recovery. This is not strictly necessary, as RF focusing will provide adequate beam envelope control during energy recovery. It is introduced to simplify installation of upgrades, which, due to reduced RF focusing at higher energy, require extra matching.

Beam viewers based on optical transition radiation (OTRs) and electromagnetic beam position monitors (BPMs) provide diagnostic information throughout the machine [9]. A diagnostic is placed approximately every quarter betatron wavelength. Air-core dipoles are placed adjacent to the diagnostics for orbit correction and diagnostic steering. The wiggler-to-arc transport and FODO backleg are instrumented to support studies investigating CSR effects [10]. Bunch arrival time/beam phase monitors are placed before and after the cryomodule for measurement and correction of transport system path lengths and momentum compactions.

The beam path footprint lies within a rectangle 5.75 m by 48 m. Table 2 provides a component summary for the driver transport system from back end of injector quarter-cryomodule to reinjection point.

Table 2: Transport System Components

Line	Bends	Quads	6-poles	H/V correctors	BPM/OTR
Injection line	3	4	0	4/4	2/3
Match to wiggler	7	6	0	3/3	3/6
Match to recirc.	4	6	0	3/3	3/3
Recirculation	10	21	8	16/11	19/8
Reinjection match	2	4	0	2/2	2/0

4 SYSTEM PERFORMANCE

4.1 Linear Optics

Figure 2 displays beam envelopes and dispersions from injection through the cryomodule during energy recovery. They are everywhere well behaved, implying that error sensitivities will be low and that apertures available in standard Jefferson Lab cavities (70 mm) and quadrupoles (54 mm) will be adequate to transport beams of the design emittance (13 mm-mrad, normalized) with low losses. BBU threshold estimates based on lattices of this character indicate that such instabilities will be avoided [11].

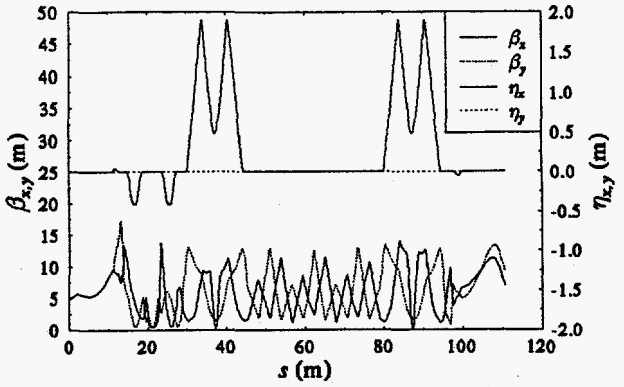

Figure 2: Driver beam envelopes and dispersions.

4.2 Aberration Analysis

Second-order aberrations are modest; good behavior is thus expected. The T_{336}, T_{346}, T_{436}, and T_{446} chromatic aberrations for transport from wiggler to reinjection point are of concern. These couple to steering errors at the wiggler to produce dispersive effects at reinjection leading to spot growth. Effort was made to limit their values to order 100 (m/(m-rad) for T_{336}, m/rad^2 for T_{346},...) or smaller; this, coupled with the stringent steering (~30 μm/30 μrad) to give electron beam/optical mode overlap required for FEL operation [12], will limit spot growth at reinjection to order 1 mm or less.

Higher-order aberration analysis was performed using various numerical tools. To certify the calculations, the principal design tool, DIMAD [13], was compared to the higher-order model TLIE [14]. Simulations showed the two codes to be generally consistent [15]. Nonlinear effects beyond second order were found to be significant and were modeled in qualitatively similar fashion by both programs.

4.3 Chromatic Performance

Chromatic performance has been investigated in detail to ensure large momentum acceptance. Momentum scans of lattice and beam properties have been performed for the module-to-wiggler and wiggler-to-module transports. System behavior is adequate over a 6% momentum range. We observe a significant variation of phase advance with momentum. This is not a serious problem in this single-pass system, but can give rise to phase space distortions in certain cases, one of which will be described during a following discussion of energy recovery. Typical system performance is shown in Figure 3, which displays a horizontal beam envelope momentum scan from wiggler to reinjection point. Note that no untoward chromatic variations are observed. Worst-case variations yield peak beam envelopes of ~35 m, a factor three times the nominal peak of order 13 m and well within the system acceptance.

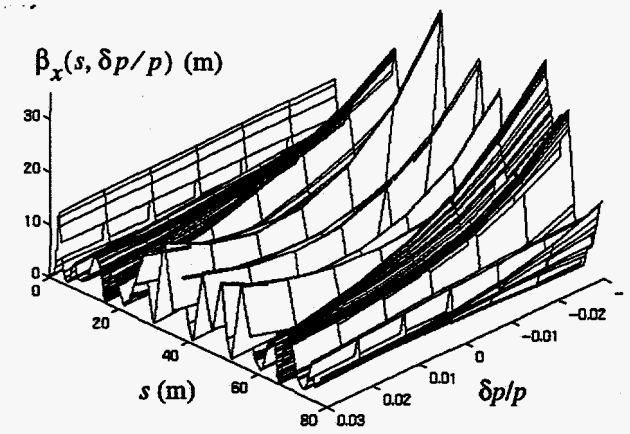

Figure 3: Momentum scan of horizontal beam envelope from wiggler to reinjection point.

4.4 Geometric Performance

Geometric aberrations have also been studied in detail. Ray-tracing simulations at a normalized emittance of 130 mm-mrad (10 times the design rms value) show only modest phase space distortion ($\Delta\varepsilon/\varepsilon \leq 0.3$) over the full momentum acceptance of the system. Figure 4 presents an image at the reinjection point of 130 mm-mrad transverse phase spaces launched at the wiggler with various momentum offsets between -3% and +3%; little phase space distortion and only modest beam envelope variations are visible.

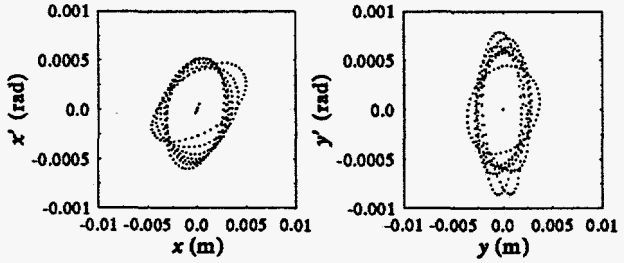

Figure 4: Geometric aberration analysis ray-trace results.

These analyses have similarly shown the system exhibits little betatron phase variation with amplitude. We therefore conclude that the geometric performance of this beamline is acceptable to at least 10 times the nominal emittance. This result holds for simulations using either equal or unequal horizontal and vertical initial emittance, implying the system exhibits little inherent horizontal/vertical coupling as well.

4.5 Simulation of Energy Recovery

Energy recovery has been simulated (without space charge) to verify lattice performance. An initial 6-sigma/6-dimensional phase space was gaussian-loaded at the center of the wiggler with 10000 particles using design beam envelopes, emittances, and a 1% rms momentum spread. This population was ray-traced to 10 MeV after the cryomodule. Figure 5 shows the resulting phase spaces; the upper plots show the phase space for ideal transport; the lower show the same data with a 1 mm initial vertical offset of the beam. We observe growth of the vertical phase space due to the aforementioned T_{336} aberration/chromatic variation of the vertical phase advance with momentum. We note that FEL operation requires steering to an orbit error of ~30 μm to ensure overlap of the electron beam and optical mode [16]; under these circumstances, the resulting spot size growth will be negligible.

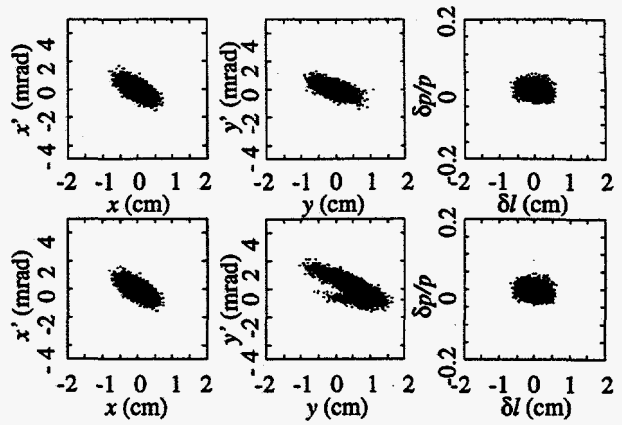

Figure 5: Ray-trace simulation of energy recovery. Upper row: ideal transport; lower row: 1 mm injection error in y.

5 ERROR EFFECTS

Error effects have been studied to develop component specifications and evaluate machine sensitivities. An aggressive project schedule has led us to explore error effects analytically and generate an "error budget", which was subsequently to be verified numerically. During energy recovery, the beam can occupy 1/3 to 1/2 of the machine physical aperture; we therefore require that beam size growth due to all known error sources be limited to ~10% of the nominal spot size. Analysis of the effect of any single error source was used to set tolerances that ensure beam spot growth is limited to the 0.1–1% range. A sum in quadrature over all errors will then be limited as desired. Simulations are being used to certify that this budget is sufficient (though perhaps more conservative than necessary) to meet machine performance targets. Error tolerances characteristic of the recirculation transport are given in Table 3.

Table 3: Typical Error Tolerances for System Components

Error		Dipole	Quad	Comments
Alignment		1 mm	0.5 mm	rms transverse
Excitation	DC	10^{-3}	10^{-3}	DC rms field error
	AC	10^{-5}	10^{-4}	rms AC "ripple"
Field quality	$\Delta B/B$	10^{-4}		variation over aperture
	$\Delta B/B$		10^{-3}	error at half aperture
	K_1	0.27 ± 0.05		end-field rolloff integral

We find that the system response to errors is generally similar to, or weaker than, that of the CEBAF linac, confirming the suitability of using standard Jefferson Lab components. The transport dipoles are an exception to this rule. In these magnets, the bend angles, dispersions, and

beam size are large; good field control and quality are needed. Effort was expended to ensure that dipole fields are uniform throughout the magnet working aperture, end-fields are well characterized, and power supply regulation is adequate to avoid ripple-driven beam quality degradation. All main dipoles will be excited in series to suppress ripple effects. A program of magnet prototyping and measurement has led to designs that provide stray field control and well-defined end-field rolloff. Information from this prototype effort [17] has been incorporated into the transport system optical design. Optics designs were done using the TRANSPORT second-order fringe-field model [18] with $K_1 = 0.27$ (based on field maps of a prototype) and K_2 neglected.

Most analytically derived tolerances were confirmed numerically. Simulations indicate a baseline array of BPMs, OTRs and steerers placed roughly every quarter wavelength in betatron phase will allow machine operation in the presence of the anticipated errors and avoid beam quality degradation. Figure 6 displays orbits from wiggler to reinjection point before and after correction for on- and off-momentum transport of ten randomly selected error sets consistent with the error budget.

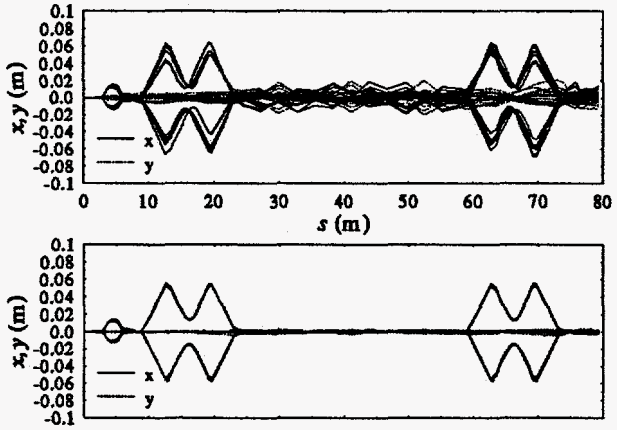

Figure 6: Orbits with errors before (top) and after (bottom) correction on and off momentum (at ±3 %).

For each "random seed", the simulations examined correction of the central orbit and all performance criteria discussed in Section 4, including chromatic behavior of the orbit (off-momentum orbits, dispersions, and momentum compactions) and beam behavior about the orbit (beam and lattice properties), large amplitude behavior (geometric aberrations and phase space distortion), and horizontal/vertical coupling. All simulations indicate that machine performance is acceptable for errors within the error budget. Studies are ongoing and will be extended to include field inhomogeneities in magnets and cavities, and to model space charge effects through the full acceleration and energy recovery cycle. The focus will then shift to commissioning and operational processes such as alternate orbit-correction algorithms, dispersion/momentum compaction adjustment, lattice/beam phase space matching, error resolution, and correction of lattice properties

6 ACKNOWLEDGMENTS

The work reported here reflects the effort of all members of the Jefferson Lab FEL Team and Accelerator Design Department. I would like to thank Dr. Fred Dylla, Dr. Court Bohn, and Dr. Joe Bisognano of Jefferson Lab for their support and guidance, and Dr. Jay Flanz of the Northeast Proton Therapy Center at Massachusetts General Hospital for considerable design assistance. This work was supported by U.S. DOE Contract DE-AC05-84ER40150.

7 REFERENCES

[1] C. L. Bohn on behalf of the Jefferson Lab FEL team., "Recirculating Accelerator Driver for a High-Power Free-Electron Laser: A Design Overview," these proceedings.

[2] S. Benson and the Jefferson Lab FEL Team, "An Overview of the Jefferson Lab IR FEL Program," presented at the 18th International Free Electron Laser Conference, Rome, August 1996.

[3] H. Liu, J. Bensch, S. Benson, J. Bisognano, D. Douglas, G. Neil, D. Neuffer, C. Sinclair, and B. Yunn, "Modeling of Space Charge Dominated Performance of the CEBAF FEL Injector," *Nucl. Instrum. and Methods A* 358 (1995) 475–478.

[4] B. Yunn, unpublished.

[5] R. Li, C. Bohn, and J. Bisognano, "Shielding Effect on the Transient Self-Interaction of a Bunch Entering a Bend," these proceedings.

[6] L. Merminga, J. J Bisognano, and J. R. Delayen, "Energy Stability in Recirculating, Energy Recovering Linacs in the Presence of an FEL," in the Proceedings of EPAC 96; L. Merminga, G. A. Krafft, D. X. Wang, and B. C. Yunn, "Longitudinal Beam Dynamics with Space Charge in an FEL Driver Accelerator," these proceedings.

[7] H. Liu, private communication; B. Yunn, unpublished.

[8] J. B. Flanz and C. P. Sargent, "Operation of an Isochronous Beam Recirculation System," *Nucl. Instrum. and Methods A* 241 (1985) 325–333.

[9] G. A. Krafft, K. Jordan, D. Kehne, J.-C. Denard, P. Piot, S. Benson, E. Feldl, J. Song, and R. Ursic, "Electron Beam Diagnostics for Jefferson Lab's High-Power Free Electron Laser," these proceedings.

[10] C. L. Bohn *et al.*, *op. cit.*

[11] B. Yunn, unpublished.

[12] S. Benson and G. Neil, private communication.

[13] R. V. Servranckx, K. L. Brown, L. Schachinger, and D. Douglas, "Users Guide to the Program DIMAD," SLAC Report 285 UC-28 (A), May 1985.

[14] J. van Zeijts and F. Neri, "The Arbitrary Order Design Code TLIE 1.0," in the Proceedings of the Workshop on Nonlinear Effects in Accelerators, IOP Publishing (1993).

[15] R. Li, unpublished.

[16] S. Benson and G. Neil, *op. cit.*

[17] J. Karn, G. Biallas, A. Guerra, and L. Harwood, "Magnetic Measurements of the Prototype Dipole for the IR-FEL at the Thomas Jefferson National Accelerator Facility," these proceedings.

[18] K. Brown, "A First- and Second-Order Matrix Theory for the Design of Beam Transport Systems and Charged Particle Spectrometers," SLAC Report 75, June 1982.